Thaumasite Formation in Hydrated and Carbonated C_3S Pastes

M.T Blanco-Varela[1*]; J. Aguilera[2], L. Trusilewicz[1]; S. Martinez-Ramirez[1]
[1]Eduardo Torroja Institute for Construction Science, (CSIC) Madrid, Spain. [2]Cementos El Monte, Huelva, Spain

Abstract

The present paper reports on a study of C_3S paste-induced generation of expansive thaumasite in C-S-H gels. The composition of the synthetic cements used was: C1- C_3S (90%) + gypsum (10%); C2- C_3S (75%) + SiO_2 gel (15%) + gypsum (10%); C3-C_3S (65%) + $CaCO_3$ (10%) + SiO_2 (15%) + gypsum (10%).

After curing for 3 months at 21 ºC, the specimens were carbonated and stored in distilled water at 5±2 ºC for 7 years. Samples were periodically monitored using XRD, FTIR, SEM/EDX and MAS NMR techniques, and tested for compressive strength. The chief conclusions were:- At terminus, the "C1" specimens had deteriorated, while the others appeared to be sound. - The expansive salt formed in the portlandite-containing "C1" specimens was thaumasite. - The Ca/Si ratio in the C-S-H gel was higher in paste "C1" than in the other two pastes. - The C-S-H gel in the seven-year C1 sample consisted primarily of linear chains of silicates, while the gel in the seven-year samples of pastes C2 and C3 exhibited a more complex structure.

Key words**:** Thaumasite; C-S-H gel, Carbonation

1. Introduction

Thaumasite is a complex calcium salt whose stoichiometric formula is: $CaO{\cdot}SiO_2{\cdot}CaSO_4{\cdot}CaCO_3{\cdot}15H_2O$. The silicon in its structure is found in the centre of a partially distorted octahedron [$Si(OH)_6$] whose OH groups are distributed asymmetrically [1]. Its formation is associated with the sulphate attack on Portland cement mortars and concretes. More specifically, in the presence of carbonate ions, sulphate ions attack the C-S-H gel produced during cement hydration. With today's widespread use of different types of cement additions, C-S-H gel composition, structure and microstructure varies and the possible effect of such variations on the risk of thaumasite-mediated deterioration is not fully understood. According to [2], slag additions reduce thaumasite formation, although [3], comparing the performance of CEM I, CEM III and CEM IV cement mortars, found the CEM III mortars (containing slag additions) to perform the worst. Furthermore, while the presence

* Instituto de Ciencias de la Construcción Eduardo Torroja (CSIC), C/Serrano Galvache 4, 28033 Madrid (Spain)

of carbonates is acknowledged to be requisite to thaumasite formation, there is some controversy about their role in the process. Kakali et al. [4] studied thaumasite formation in cement specimens with limestone filler additions, finding their presence to enhance the formation of the salt. Other authors [5, 6], however, have reported the contrary. Blanco-Varela et al. [7, 8], in turn, proved that sufficient carbonates are produced during mortar carbonation for thaumasite attack to take place.

The purpose of the present study was to determine the capacity of C_3S pastes to generate expansive thaumasite in C-S-H gels. The approach taken was to conduct an analysis of thaumasite formation from the C-S-H gels obtained by hydrating synthetic C_3S in the presence and absence of amorphous SiO_2 and different sources of $CaCO_3$.

2. Experimental

C_3S was synthesized from a mix of stoichiometric quantities of $CaCO_3$ and SiO_2; the synthesized phase was XRD-tested for purity. Three synthetic cements were made from C_3S, amorphous SiO_2, gypsum and $CaCO_3$, varying the composition as follows: C1- (90%)C_3S + (10%)gypsum; C2- (75%)C_3S + (15%)SiO_2 + (10%)gypsum; C3- (65%)C_3S + (15%)SiO_2 + (10%)gypsum + (10%)$CaCO_3$. These cements were mixed with different amounts of water in order to get pastes with the same workability (water/cement ratio = 0.9 for C1 and C2 and 0.8 for C3). Pastes were used to prepare 200 cylindrical specimens measuring 1 cm in diameter by 1 cm high. After curing for 3 months at 21 ºC and 100% RH, the specimens were subjected to two weeks of accelerated carbonation in a CO_2 chamber containing a hygroscopic salt to keep the relative humidity at around 50%. Finally the specimens were stored in distilled water at 5 $\pm$ 2 ºC for up to seven years.

The pastes were characterized for mineralogy with FTIR, XRD and DTA/TG; for microstructure with Hg porosimetry; and for strength with compressive testing, at the following stages: end of hydration; end of carbonation; during the first year, approximately every three months after immersion in H_2O at a temperature of 5 ± 2 ºC; and once a year thereafter. After seven years, XRD, FTIR, SEM/EDX and ^{29}Si MAS NMR analyses were run to determine paste mineralogy.

SEM analysis were carried out in a Jeol 4500 microscope, working at 20KV and being sample distance 20 mm. Fracture surface was covered by carbon sputtering. Microanalyses were performed in an EDX Oxford-Link System ISI.

3. Results

3.1 Mechanical strength and porosity

Table 1 shows the mechanical strength and porosity for the hydrated paste specimens after carbonation and storage in water for different periods of time. While paste strength was not high after hydration, porosity was, due in all likelihood to the high w/c ratio used in the mix. Carbonation, in turn, raised mechanical strength substantially and lowered porosity in the three pastes. No significant change was observed in the strength of specimens stored in water until the age of 30 months. Pastes C2 and C3 exhibited similar strength after seven years, whereas the paste C1 specimens were cracked and deformed due to expansion (Figure 5A). Specimen porosity increased significantly at this age.

Table 1 Paste mechanical strength and porosity at different ages

	Mechanical strength (MPa)							Porosity (% vol.)				
	Hy	Car	3M	5M	15M	30M	7Y	Hy	Car	3M	5M	7Y
C1	9,6	40	29,3	27,4	28,4	25	-	37,3	11,9	14,5	12,5	14,6
C2	4,3	15,4	16	16	20	15	17	41,7	29,1	26,3	27,9	32,4
C3	2,4	9,6	14,4	12,4	10,1	8,4	9,6	43,7	40,18	24,6	29,6	33,5

Hy= hydrated; Car=carbonated; 3M, 5M, 15M, 30M = 3, 5, 15, 30 months of curing in water, respectively; 7Y = 7 years of curing in water

3.2 Infrared spectroscopy (FTIR), X-ray diffraction (XRD)

Figure 1A shows the FTIR spectra for the three hydrated pastes and the spectrum for paste C1 after carbonation. Table 2, in turn, gives spectrum band position and assignment. The spectra for the three pastes after 5 and 15 months and 7 years of curing in water at 5 ± 2 ºC are given in Figure 1B.

The spectra for the three hydrated pastes (Figure 1A) are very similar. The results for paste C1 shows an intense νOH band at 3640 cm^{-1} from portlandite that is barely visible in the paste C2 and completely non-existent in the paste C3 spectrum. This is in an indication that in cements C2 and C3 a pozzolanic reaction took place between the portlandite formed during C_3S hydration and the SiO_2 gel. The gypsum as well as the C-S-H gel bands (bands 12, 22 and 24 in Table 2), which are not affected by the pozzolanic reaction, are very similar. The samples are somewhat carbonated, exhibiting the characteristic wide $\nu_3 CO_3$ vibration bands attributed to scantly crystalline carbonates – which are narrower in paste C3.

When the specimens are carbonated (such as C1 in Figure 1), the portlandite and gypsum bands (except the peak at 669 cm^{-1}) disappear, while new bands attributable to calcite, aragonite, vaterite and even amorphous carbonates appear. The bands due to silicate vibrations in the C-S-H gel, in turn, shrink considerably, a new band appears at 1080 cm^{-1} and the band at 456 shifts to 468 cm^{-1}. All this is indicative of intense C-S-H gel carbonation and the presence of silica gel [17]

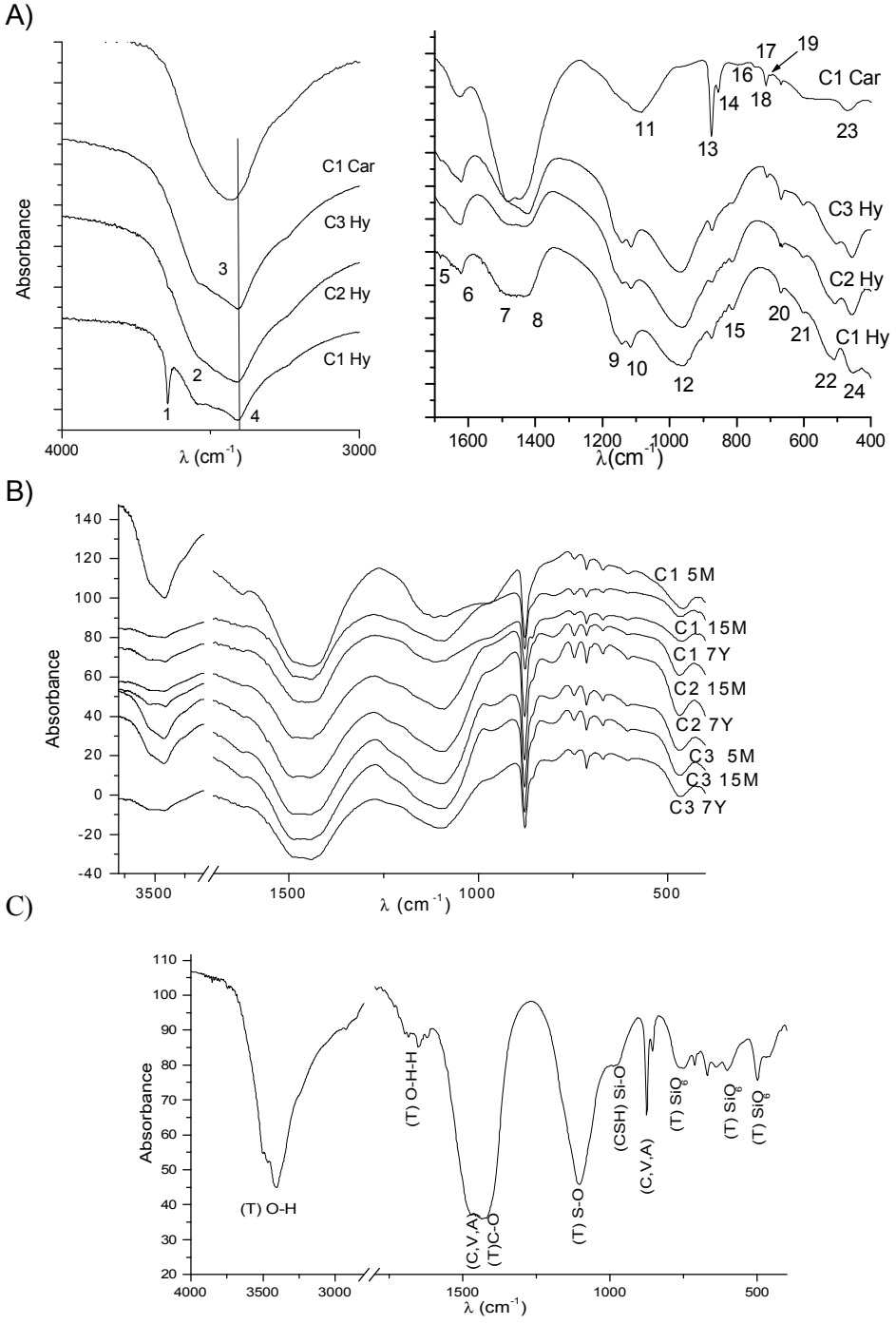

Figure 1. FTIR spectra. A) for the hydrated pastes and carbonated C1 paste. B) for pastes after 5 and 15 months and 7 years curing. C) of the thaumasite found in cracks and fractures in seven-year C1 samples (T = thaumasita, V= vaterita, A= Aragonite, C = Calcite)

After storage in water for five months (Figure 1B), paste C1 hydration progresses, with the concomitant intensification of the C-S-H gel bands. In this same period, gypsum recrystallizes and its bands re-

appear on the spectra, the calcite and vaterite bands grow and the aragonite peaks decline. The FTIR spectra for C2 and C3 are very similar from five months through terminus.

A decrease in absorption is observed at around 970 cm^{-1} (due to Si-O bond stretching vibrations in the C-S-H gel) in the paste C1 7Yspectra.

Table 2. FTIR bands for the hydrated pastes and carbonated paste C1.

λ (cm^{-1}) (No.)	C1 Hy	C2 Hy	C3 hy	C1 car	Assigned to	Comments
3643 (1)	xxx	o	--	--	OH strch	OH in Portlandite
3546 (2)	xx	xx	xx		OH symm. strchng	H_2O Gyp. cryst.
3435 (3)	--	--	--	xxx		
3405 (4)	xx	xx	xx			
1684 (5)	xx	xx	xx		H-O-H Bending	H_2O Gyp. cryst.
1625 (6)	xx	xx	xx	x		
1480 (7)	x	x	x	xxx	ν_3 CO_3	$CaCO_3$am,Arag. Vat
1440 (8)	x	x	xx	xxx		Calcite
1144 (9)	xx				ν_3 SO_4	Gypsum
1116 (10)	xx					
1088 (11)	--	--	--	xxx	ν_3 SiO_4	Silica gel
969 (12)	xxx	xxx	xxx	o		C-S-H
876 (13)	x	x	x	xx	ν_2 CO_3	Calc. Vat. C_3S
855 (14)				x		Aragonite
813 (15)	x	x	x			C_3S???
796 (16)	--	--	--	x	Si-O symm. strchng	SiO_2 gel
745 (17)	--	--	--	o	ν_4 CO_3	Vaterite
712 (18)	--	--	x	x		Calc. Arag. Vat.
700 (19)				o		aragonite
669 (20)	x	x	x	x	ν_4 SO_4	Gypsum
602 (21)	x	x	x	-		
512 (22)	xx	xx	xx	o	ν_2 SiO_4	C-S-H
468 (23)	--	--	--	xx		
455 (24)	xx	xx	xx	--		C-S-H

Calc = calcite; Arag= aragonite; Vat = Vaterite;Gyp =Gypsum; strtchng = stretching; symm. = symmetric; a-sym. = antisymmetric; - = absence; o = trace; x = low intensity; xx = medium intensity; xxx = high intensity

A white powder was observed in the areas around the cracks in the seven-year paste C1 specimens. Some of the bands on its FTIR spectrum (Figure 1C) can be assigned to thaumasite [9].

The diffractograms of the pastes confirm the existence of the same crystalline phases as observed with FTIR and exhibit high background and weak reflection intensities, with a halo at 29-32º indicative of amorphous phases not detectable with XRD technique.

3.3 Differential thermal and thermogravimetric analysis (DTA/TG).

At temperatures of up to 200 ºC, the DTAs of the hydrated samples (Figure 2) contain two endothermal signals. The peaks at around 112-118 ºC in the first are due to partial dehydration of the gypsum and the C-S-H gel, as well as to some unbound water in the pores of the material. The second signal, with peaks at around 140-145 ºC, is due to the dehydration of calcium sulphate hemihydrate. An endothermal signal due to portlandite dehydroxylation appears at around 450-500 ºC. This signal is more intense in hydrated paste C1 than in C2 Hy or C3 Hy, indicating that an intense pozzolanic reaction took place in the latter two. Finally, the endothermal band at temperatures of over 700 ºC is due to sample decarbonation. In pastes C1 and C2 this signal, visible at a lower temperature than in paste C3, corresponds to scantly crystalline carbonates produced as a result of reactions with atmospheric CO_2 during sample handling. It is more intense and appears at a higher temperature in paste C3, which contained 10% $CaCO_3$ in the form of calcite.

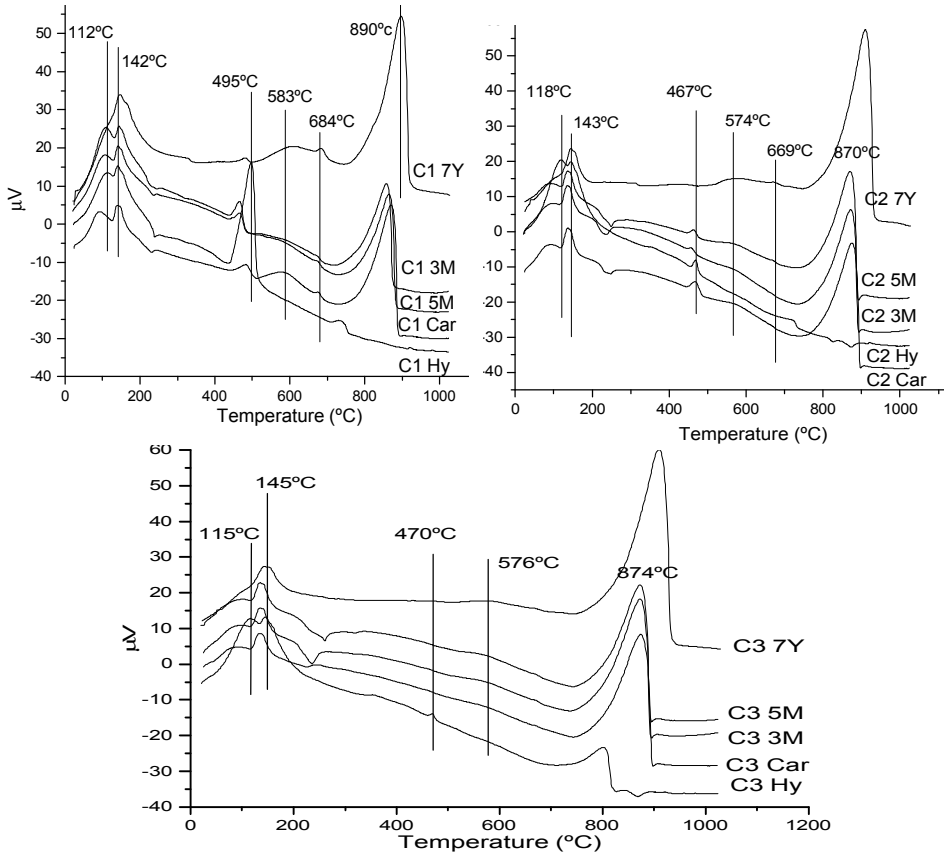

Figure 2. Paste DTAs at different test times

The decline in intensity and maximum temperatures observed in the first two endothermal peaks on the DTAs for the carbonated samples is interpreted to reflect the descending amounts of C-S-H gel and gypsum in the samples as a result of carbonation. A reduction is observed in the portlandite peak (particularly in the paste C1 curve; in the C3 curve

it disappears altogether), along with a steep rise in the $CaCO_3$ endothermal decarbonation signal. Finally, two endothermal signals appear in all three curves but especially in the paste C1 curve: a wide first peak at 570-585 ºC and a narrower one at 664-670 ºC whose nature is unclear but which is associated with weight loss.

The DTA signals vary fairly little with time, although gypsum recrystallizes and the dehydration signal grows more intense; a tiny portlandite dehydroxylation signal is still visible in the seven-year paste C1 curve but in neither of the other two; the former thermogram contains a shoulder on the second endothermal peak at around 164 ºC that may be attributed to thaumasite dehydration [10].

Table 3 shows paste weight loss in per cent, (normalized against initial weigth), versus temperature. The percentage of $CaCO_3$ in the samples was calculated assuming that between 700 and 950 ºC the only CO_2 lost was from the $CaCO_3$; the portlandite percentage, in turn, was calculated by running DTG on the samples and selecting the most appropriate range of temperatures for each case. The Ca/Si ratios for the C-S-H gels in the pastes were computed assuming that with the exception of the gypsum, $Ca(OH)_2$ and $CaCO_3$ all the Ca in the samples, and all the Si in the samples without exception, are contained in the C-S-H gel.

Table 3. Paste weight loss at different temperatures and test ages

T	C1 (wt%)						C2(wt%)				
(ºC)	Hy	Car	3M	5M	7Y		Hy	Car	3M	5M	7Y
100	2.6	2.4	3.2	2.5	1.3		3.4	1.9	1.5	1.7	0.9
150	6.2	4.4	6.7	5.5	3.8		8.9	3.5	3.0	3.3	2.1
180	7.6	5.0	7.9	6.5	5.0		10.9	3.7	3.2	3.5	2.5
420	11.3	6.8	10.9	9.2	7.8		15.8	4.8	4.2	4.8	3.3
520	16	8.1	12.1	10.4	8.7		17.3	5.6	5.1	5.8	3.9
700	17.4	14.7	16.4	15.3	13.7		18.9	9.6	9.6	10.7	6.8
950	19.7	35.9	33.6	35.2	34.6		20.3	33.8	33.6	34.0	33.4
Por	19.6	3.6	3.6	2.8	2.4		3.8	2.3	2.3	2.9	0.8
Cal	5.1	48.2	39.1	45.1	47.6		3.1	54.9	54.5	52.8	60.5
C/S	2.02	0.94	1.36	1.12	1.07		1.60	0.25	0.27	0.28	0.17
C/S*					1.52						0.73
	C3 (wt%)										
100	3.2	1.7	1.4	1.3	0.9	TºC					
150	8.1	3.0	2.8	2.6	2.3	700	17.4	9.2	9.9	9.7	7.0
180	9.9	3.2	2.9	2.8	2.8	950	23.4	34.8	34.4	34.7	34.2
420	14.3	4.2	4.1	4.1	4.3	Por	2.1	0	0	0	0
520	15.6	5.0	5.0	5.0	4.4	Cal	13.5	58.1	55.8	56.8	61.7
C/S	1.49	0.27	0.34	0.31	0.18	C/S*					0.59

Por = Portlandite; Cal = $CaCO_3$; C/S= Ca/Si in the C-S-H gel; C/S*= Ca/Si in the C-S-H gel, corrected for NMR results

The TGA data for the three hydrated pastes confirmed the greater abundance of portlandite in paste C1 and its uptake in the pozzolanic reaction with the SiO_2 gel in pastes C2 and C3. The losses at 420 ºC

were also observed to be much higher in pastes C2 and C3 than in C1. Given, moreover, that such losses corresponded to the chemically combined water in the gypsum and C-S-H gel and that all samples had the same gypsum content, it may be concluded that hydrated pastes C2 and C3 had more C-S-H gel than paste C1.

Nearly all the portlandite is transformed into $CaCO_3$ during carbonation, but the high percentages of $CaCO_3$ in the carbonated samples cannot be explained solely by the portlandite content in the hydrated samples. Consequently, some Ca must also come from the C-S-H gel. The steep decline in losses at 420 ºC in all three carbonated pastes with respect to the respective hydrated pastes confirms that there is less water bound to the C-S-H gel structure. These data are consistent with the FTIR findings.

The TGA studies also indicate that pastes C2 and C3 are more highly carbonated than paste C1 and that carbonation rises, although only slightly, with curing time. The thermograms for the carbonated cement C1 pastes stored in water for three months show a further increase in loss at 420 ºC. This may be interpreted to signal an increase in the amount of C-S-H gel due to hydration of the anhydrous C_3S in the sample and to gypsum recrystallization, both consistent with the FTIR results. By contrast, the thermograms for similar pastes made with cements C2 and C3 barely show any variation with time.

Finally, at temperatures of from 520 to 700 ºC (associated with endothermal DTA signals), substantial weight losses were recorded in the thermograms for all the carbonated pastes at all test times. Greater losses were observed in paste C1 than in C2 or C3. This may be the result of loss of CO_2 in amorphous carbonates bound to the C-S-H gel or of water in the silanol groups found in the silica gel carbonation product, which remain stable over time.

3.4 Nuclear magnetic resonance (^{29}Si MAS NMR)

The ^{29}Si MAS NMR spectra for the three pastes after seven years of curing are shown in Figure 3 and the results of deconvoluting the signals are found in Table 4. The spectrum for sample C1, to which no SiO_2 was added, contains a small signal attributed to monomeric silicate at -72 ppm due to the presence of residual anhydrous C_3S. The most intense bands, at -79 ppm and -85 ppm, are attributed to the Q^1 and Q^2 units on the silicate chains in the C-S-H gel formed during C_3S hydration [11]. This spectrum also has less intense bands at -92 ppm, -101 ppm and -111 ppm attributed to Q^3 and Q^4 silicate units. Both are products of C-S-H gel decalcification during carbonation [12], a process that may also induce C-S-H gel inter-chain bonding (Q^3 units) or even produce silica gel (Q^4 units). The signal for thaumasite octahedral silicon does not appear in these spectra because the recording conditions were unsuited to detection of this species [13].

In the spectra for samples C2 and C3, the most intense band, appearing at -112 ppm (Q^4 Si units), may be due to the unreacted portion of the SiO_2 added to the paste mix and to the silica gel produced during C-S-H gel carbonation. Both spectra also show an intense band at -102 ppm and another less intense band at -91 and -94 ppm (samples C2 and C3, respectively). These are due to Q^3 Si units in the C-S-H gel resulting from the pozzalanic reaction or possibly to cross-linked structures formed by the C-S-H gel silicate chains during carbonation [14]. Finally, the spectra for sample C3 contain a less intense band at around -86 ppm, interpreted to be due to the Q^2 units in the C-S-H gel silicate chains. The ^{29}Si CP/MAS NMR [H^+] spectra for these same samples denote the presence of Si-O-H groups associated with the signals in the Q^1, Q^2 and Q^3 zo nes, confirming the foregoing interpretations.

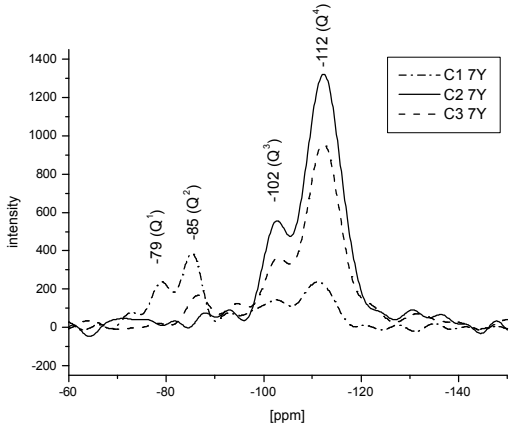

Figure 3.- ^{29}Si MAS NMR spectra for the three samples after storage in water at 5º C for seven years.

Table 4. Chemical shift and deconvolution of the ^{29}Si MAS NMR spectra for pastes after seven years of curing

Assigned	*C1 7Y*		*C2 7Y*		*C3 7Y*	
to	Δ(ppm)	wt%	δ (ppm)	wt%	δ (ppm)	wt%
Q^0	-72.84	3.46				
Q^1	-79.10	18.02				
Q^2	-85.38	28.30			-86.54	7.54
Q^3	-92.9	4.12	-91.11	5.04	-94.78	6.77
Q^3	-101.78	20.01	-102.25	18.23	-102.43	15.49
Q^4	-111.61	26.09	-112.32	76.73	-112.29	70.15

3.5 Scanning electron microscopy (SEM/EDX).

While the specimens made with pastes C2 and C3 were in good condition after seven years of immersion in water at 5º C, the ones made with paste C1 were deteriorated due to expansion (Figure 5A). SEM/EDX analysis of the fracture surface identified lanceolate crystals characteristic of aragonite (Figure 5B), needle shaped thaumasite crystals (Figures 5C and 5D) and prismatic crystals typical of gypsum (Figure 5E). Figure 5F depicts the smooth and compact structure of the

C-S-H gel, the layer of calcium carbonate surrounding its particles and the thaumasite crystals be growing on its surface.

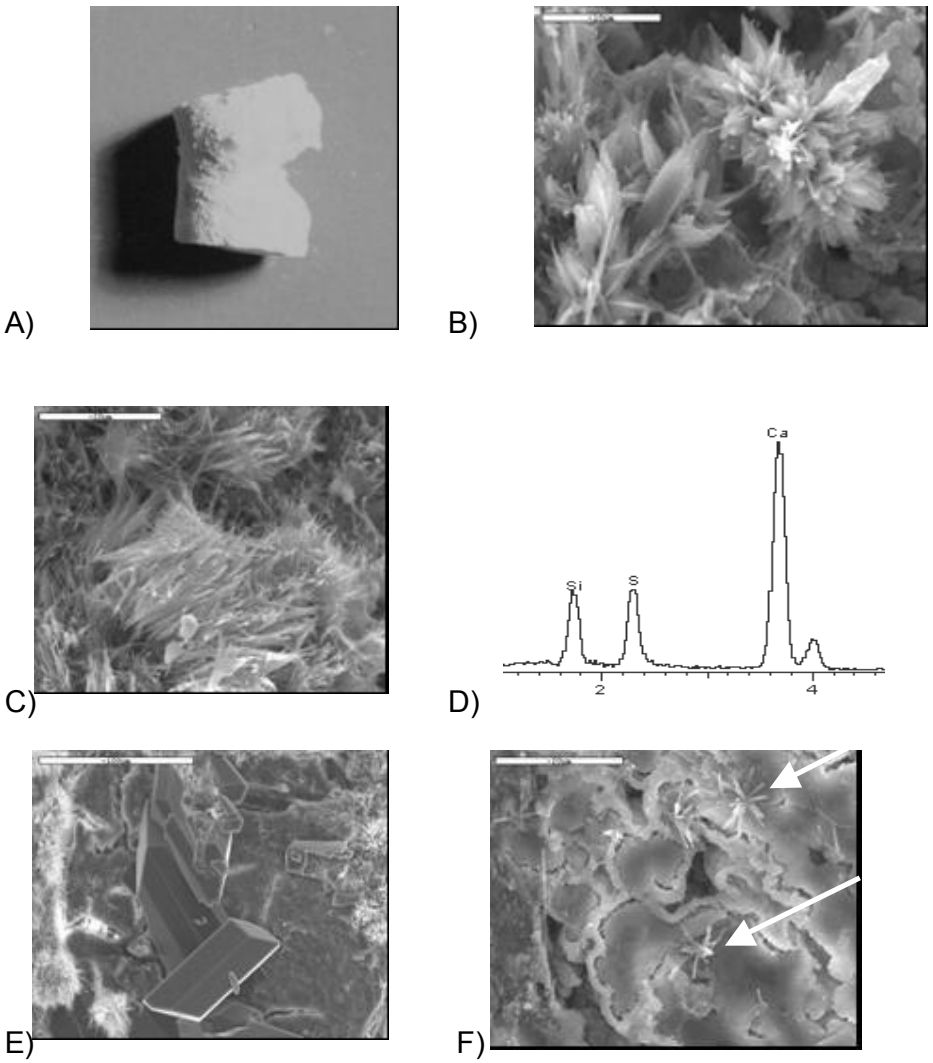

Figure 5. A) Paste C1 specimen fractured due to the expansive formation of thaumasite; B) Aragonite crystals (mark=10μm); C) Thaumasite crystals (mark=20μm); D) EDX for thaumasite crystals; E) Gypsum, calcite and thaumasite crystals (mark=100μm); F) arrows indicating Thaumasite growing on the C-S-H gel surface (mark=20μm).

The EDX spectra for the C-S-H gel indicate the existence of a small amount of S, with a variable composition and a mean molar Ca/Si ratio of 1.3 ±0.3 (data obtained as average of 15 individual analysis). No thaumasite crystals are visible on the seven-year samples of pastes C2 and C3, which do contain gypsum crystals, however, as well as $CaCO_3$ polymorphous species and SiO_2 particles. The mean Ca/Si ratio found for the C-S-H gel in sample C2 after seven years was 0.69, and for the seven-year C3 sample, 0.56 ± 0.03.

4. Discussion and concluding remarks

The hydration of the three cements – C1, C2 and C3 – gives rise to pastes with differing C-S-H gel composition, whose Ca content declines in ascending order (Table 4). Paste carbonation prompts C-S-H gel decalcification, formation of the three $CaCO_3$ poly morphs, portlandite uptake, decline in porosity and so forth.

The Ca/Si ratio in C-S-H gels (calculated fron TGA data) is higher, at all ages, in paste C1 than in pastes C2 and C3. The Ca/Si ratios in paste C2 and C3 C-S-H gel as determined by TGA are very low at all ages (after carbonation), due perhaps to the fact that not all the Si in the samples forms a part of the gels. And indeed, SEM/EDX identified particles containing only Si, with no Ca; FTIR analysis detected silica gel in the samples; and according to the NMR study, some Si formed a part of a three-dimensional SiO_4 tetrahedral structure. Consequently, inasmuch as the amount of Q^4 Si, which would not be found in C-S-H gel, was determined with ^{29}Si MAS NMR, a correction was made assuming that only the Q^1, Q^2 and Q^3 Si would form a part of the gel.

The results obtained under that assumption indicated that the C-S-H gel in the C1 7Y sample, which contained thaumasite, had a Ca/Si ratio of 1.52, while this value was 0,73 and 0,59 for C2 7Y and C3 7Y respectively. This is highly consistent with the EDX findings.

Further to Bellman's [15] calculations, thaumasite can feasibly be formed from C-S-H gel or $Ca(OH)_2$ and SiO_2 in the presence of gypsum and $CaCO_3$; the presence of $Ca(OH)_2$ is not necessary in the former case. Since the three pastes studied contained $CaCO_3$, gypsum and C-S-H gel after seven years of testing, thaumasite could have formed in any or all of them. And yet the salt was identified in the seven-year C1 sample only. The quantity, structure and composition of C-S-H gel may, then, be thought to affect its reactivity with sulphates and carbonates to form thaumasite.

The C-S-H gel in seven-year sample C1 was richer in calcium than the gel in samples C2 and C3 and consisted primarily of linear chains of silicates, while the gel in seven-year samples C2 and C3 was more highly decalcified. Moreover, sample C2 had no linear silicate chains in its structure and sample C3 a much smaller proportion than sample C1. The only seven-year paste containing a small quantity of portlandite was sample C1. This salt is compatible with Ca-rich C-S-H gels but not with gels with lower contents of the element or with SiO_2 gel. As portlandite releases Ca^{2+} and OH^- ions into the system, the thaumasite solubility product would be more readily attained [16]. In addition, according to the NMR results, the amount of Si forming a part of the gel in C1 doubled the amount in C2 and C3. Hence, the amount of C-S-H gel in sample C1 was much greater than in the other two pastes. This would also favour thaumasite formation. It would appear therefore that

although thaumasite may form across a wide range of concentrations in the CaO-SiO_2-$CaCO_3$-$CaSO_4$-H_2O system [16], it is more readily formed in the CaO-rich areas of the system, i.e., in the presence of portlandite and where Ca-richer C-S-H gels are stable.

Thaumasite has been only formed from C-S-H gel of Paste C1 7Y. That gel has higher Ca/Si ratio and more lineal structure than those of C2 7Y and C3 7Y pastes. Paste C1 7Y contain more amount of C-S-H gel than the other two, and it is the only paste containing portlandite. Then it seems that quantity, structure and composition of C-S-H gel can play important role in thaumasite formation.

5. Acknowledgements:
This research was funded by the Spanish MCYT and UE under projects MAT2003-08343 and MEST-CT2004-513915 respectively. S. Martínez benefited from a "Ramón y Cajal" contract financed by the MCYT and the EU.

6. References

[1] R.A. Edge, H.F.W. Taylor. Crystal structure of thaumasite, $[Ca_3Si(OH)_6 12H_2O](SO_4)(CO_3)$. Acta Crystallography B27: (1971) 594-601.
[2] P.W. Brown, R.D. Hooton, B.A. Clark, The co-existence of thaumasite and ettringite in concrete exposed to magnesium sulfate at room temperature and the influence of blastfurnace slag substitution on sulfate resistence. Cem. Con. Com. 26 (2004) 993-999.
[3] M.T. Blanco-Varela; S. Martinez-Ramirez; F. Adeva; I. Pajares "Influence of cement type in thaumasite formation" 6th International Congress Global Construction: Ultimate Concrete Opportunities. Ed. Ravindra K. Dhir. (Thomas Thelford). Dundee U.K.2005, Vol 6, 749-755.
[4] G. Kakali, S. Tsivilis, A. Skaropoulou, J.H. Sharp, R.N. Swamy, Parameters affecting thaumasite formation in limestone cement mortar Cem. Con. Comp.25 (2003), 977-981
[5] J. Zelic, R. Krstulovic, E. Tkalce, P. Krolo, Durability of the hydrated limestone-silica fume Portland cement mortars under sulphate attack Cem. Con. Res. 29(6) (1999) 819-826
[6] G. Piasta, Z. Sawicz, G. Koprowski, Z Owsiak. Influence of limestonepowder filler on microstructure and mechanical properties of concrete under sulphate attack, 10th Int. Congr. Chem. Cem., Goteborg, Sweden, (1998) (4iv018 8p).
[7] M.T. Blanco-Varela, J. Aguilera, S. Martínez-Ramírez, "Effect of cement C_3A content, temperature and storage medium on thaumasite formation in carbonated mortars" Cem. Con. Res. 36(4) (2006) 707-715.
[8] J. Aguilera, S Martinez-Ramirez, I. Pajares, M.T. Blanco-Varela, Formation of thaumasite in carbonated mortars. Cem. Concr. Comp. 25 (2003) 991-996.
[9] J. Aguilera, M.T. Blanco-Varela, T. Vázquez. Procedure of synthesis of thaumasite. Cem. Concr. Res. 31 (2001) 1163-1168
[10] Bensted J., Thaumasite a deterioration product of hardened cement structures. Il Cemento, 85, pp.3-10, 1988.
[11] A.R. Brough, C.M. Dobson, I.G. Richardson, G.W. Groves. In-situ solid-state NMR-studies of Ca_3SiO_5 hydration at room-temperature and at elevated temperatures using Si-29 enrichment. J. Mat. Sci. 29 (1994) 3926-3940.
[12] N.R. Short, A.R. Brough, A.M.G. Seneviratne, P. Purnell, C.L. Page. Preliminary investigations of the phase composition and fine pore structure of super-critically carbonated cement pastes J. Mat. Sci. 39 (2004) 5683-5687.

[13] J. Skibsted, L. Hjort, H.J. Jakabsen, Quantification of thaumasite in cementitious materials by Si-29(H-1) crosspolarization magic-angle NMR spectroscopy Adv. Cem. Res. 9 (35) (1997) 135-138

[14] S. Martinez-Ramirez, M.T. Blanco-Varela, I. Ereña, M. Gener. Pozzolanicity of two zeolitics rocks from Cuba: characterization of reaction products. Applied Clay Science 32, (2006) 40-52.

[15] F. Bellmann. On the formation of thaumasite $CaSiO_3.CaSO_4.CaCO_3.15H_2O$: Part I. Adv. Cem. Res. 16 (2) (2004) 55-60.

[16] M.T. Blanco-Varela, J. Aguilera, S. Martínez-Ramírez**.** Thermodynamic compatibility of thaumasite with hydrated cement phases. 6th Int. Congress Global Construction: Ultimate Concrete Opportunities. Ed. Ravindra K. Dhir. (Thomas Thelford). Dundee UK. 2005 Vol 6, 743-748.

[17] M.Palacios, F. Puertas. Effect of carbonation on alkali-activated slag paste. J. Am. Ceram. Soc. 89 (10) (2006) 3211-3221